AD-A186 366

REPORT DOCUMENTATION PAGE

1a. REPORT SECURITY CLASSIFICATION UNCLASSIFIED	1b. RESTRICTIVE MARKINGS

DTIC SELECTED OCT 1 3 1987 C+D

2a. SECURITY CLASSIFICATION AUTHORITY	3. DISTRIBUTION/AVAILABILITY OF REPORT
2b. DECLASSIFICATION/DOWNGRADING SCHEDULE	APPROVED FOR PUBLIC RELEASE DISTRIBUTION IS UNLIMITED

4. PERFORMING ORGANIZATION REPORT NUMBER(S)	5. MONITORING ORGANIZATION REPORT NUMBER(S)
	AFOSR·TR· 87-1269

6a. NAME OF PERFORMING ORGANIZATION PRINCETON UNIVERSITY	6b. OFFICE SYMBOL (If applicable)	7a. NAME OF MONITORING ORGANIZATION AFOSR/NA

6c. ADDRESS (City, State and ZIP Code) PRINCETON, NJ 08544	7b. ADDRESS (City, State and ZIP Code) BUILDING 410 BOLLING AFB, DC 20332-6448

8a. NAME OF FUNDING/SPONSORING ORGANIZATION AFOSR/NA	8b. OFFICE SYMBOL (If applicable) NA	9. PROCUREMENT INSTRUMENT IDENTIFICATION NUMBER AFOSR 85-0126

8c. ADDRESS (City, State and ZIP Code) BUILDING 410 BOLLING AFB, DC 20332-6448	10. SOURCE OF FUNDING NOS			
	PROGRAM ELEMENT NO. 61102F	PROJECT NO. 2307	TASK NO. A2	WORK UNIT NO.

11. TITLE (Include Security Classification) (U) FUNDAMENTAL ASPECTS OF THE STRUCTURE OF SUPERSONIC TURBULENT BOUNDARY LAYERS

12. PERSONAL AUTHOR(S) J H WATMUFF AND A J SMITS

13a. TYPE OF REPORT ANNUAL TECHNICAL	13b. TIME COVERED FROM APR 86 TO MAY 87	14. DATE OF REPORT (Yr., Mo., Day) MAY 1987	15. PAGE COUNT 40

16. SUPPLEMENTARY NOTATION

17. COSATI CODES			18. SUBJECT TERMS (Continue on reverse if necessary and identify by block number)
FIELD	GROUP	SUB GR	TURBULNECE, BOUNDARY LAYER, SUPERSONIC FLOW

19. ABSTRACT (Continue on reverse if necessary and identify by block number)

Measurements of structure angle in a supersonic turbulent boundary layer with zero and adverse pressure gradients are presented. Conditionally sampled measurements of u, v, and uv are presented along with quadrant analysis of the turbulnet fluctuations. The latter suggests ambiguities associated with the interpretation of VITA measurements. Preliminary results of experiments on artificially generated hairpin vortices are also discussed. Measurements indicate a high degree of similarity between the signatures of these hairpin structures and ensemble averaged events in the turbulent boundary layer.

20. DISTRIBUTION/AVAILABILITY OF ABSTRACT UNCLASSIFIED/UNLIMITED ☒ XX SAME AS RPT ☐ DTIC USERS ☐	21. ABSTRACT SECURITY CLASSIFICATION UNCLASSIFIED

22a. NAME OF RESPONSIBLE INDIVIDUAL JAMES M MCMICHAEL	22b. TELEPHONE NUMBER (Include Area Code) 202-767-4935	22c. OFFICE SYMBOL AFOSR/NA

DD FORM 1473, 83 APR EDITION OF 1 JAN 73 IS OBSOLETE UNCLASSIFIED

SECURITY CLASSIFICATION OF THIS PAGE

Fundamental Aspects of the Structure of

Supersonic Turbulent Boundary Layers

SECOND ANNUAL REPORT

by

Jonathan H. Watmuff and Alexander J. Smits

Mechanical & Aerospace Engineering Department
Princeton University
Princeton, New Jersey 08544

INTRODUCTION

This report is the Second Annual Report on AFOSR Contract 85-0126 "Fundamental Aspects of the Structure of Supersonic Turbulent Boundary Layers," monitored by Dr. J. McMichael. The contract has addressed three fundamental tasks. In Task A, the structure of flat plate supersonic turbulent boundary layers are being investigated under the conditions of a zero pressure gradient, and under conditions of a mild adverse pressure gradient. In Task B, longitudinal curvature effects in turbulent boundary layers are being studied. In particular, a detailed investigation is being made of the relaxation behavior of a subsonic boundary layer downstream of a short region of strong convex curvature. As a result of the work performed under these task headings, Task C has been introduced to analyze, investigate and control the behavior of simple wall-bounded vortex loops. This task is now making a major contribution to the understanding of the ensemble-averaged structure obtained in both the low and high speed turbulent boundary layers.

TASK A: THE STRUCTURE OF SUPERSONIC, TURBULENT BOUNDARY LAYERS

The principal aim of this task is to develop a physical model for supersonic turbulent boundary layer structure which can be used as the basis for improved calculations of turbulent flow. The current effort is directed towards a better understanding of the large-scale structures, that is, the energy-containing motions in the fully turbulent region, under conditions of zero and adverse pressure gradients.

At the time of the First Annual Report, April, 1986, the presence of "finger-like" structures in a zero pressure gradient boundary layer had been established. They were inclined at about 45° to the flow direction, they appeared to have a limited spanwise and streamwise extent, and they were convected downstream for considerable distances without losing their identity. These conclusions were based on measurements taken with multiple normal hot-wire probes, multiple wall-pressure transducers, and high-contrast schlieren photographs. The analysis used space-time correlations and conditional averaging using the single-point VITA technique.

Some interesting new results have been obtained since then:

(a) Eddy-angle measurements

Measurements of the structure angle (derived from the space-time correlation of the signals from two parallel wires) have been obtained for an adverse pressure gradient supersonic layer and a zero pressure gradient subsonic layer. In the supersonic case, the initial Reynolds number based on momentum thickness R was about 82,000, the static pressure rose by a factor of 1.9 in a distance of approximately $10\,\delta_0$ (δ_0 is the initial boundary layer

thickness), and the Mach number decreased from 2.85 to 2.10 in the same distance. In the subsonic case, R was much lower, and it was equal to approximately 5700. The results for the subsonic case are discussed under the heading for Task B. The adverse pressure gradient boundary layer results of Fernando and Smits (1987) are shown in Fig. 1 for two different wire separations . The results of the smaller separation wires (y/δ_o = 0.09) show that the incoming boundary layer structure angle is around 45° over most of the layer with a decrease in angle near the wall and an increase in angle near the outer edge of the layer. The structure angle can be seen to increase by approximately 5° through the interaction. Much the same results were obtained with the larger separation wires (y/δ_o = 0.18) although the structure angles are consistently higher by around 5°. These angles were calculated assuming a convection velocity equal to the mean velocity half-way between the wires. The data have recently been re-analyzed assuming a fixed (invariant with wall distance) structure convection velocity of 0.8 times the free-stream velocity. The differences in structure angles between the incoming and the adverse presure gradient boundary layers were found to be slightly smaller and of the order of the experimental uncertainty.

Two additional results have been obtained with respect to the eddy angle. First, by using VITA to detect significant events on one wire, and examining the simultaneous signal from the other wire, the variance of the eddy angle can be determined. Preliminary results have shown that the two signals typically have a correlation coefficient greater 0.95, and that the variance is of the order of 15°. Second, one wire was placed as close as possible to the wall, at $y^+ \simeq 60$, and another wire was traversed through the layer. This method of

measuring eddy angles has been tried by others, and gives very low angles throughout the layer, of order 15° to 30° (Brown & Thomas 1977, Robinson 1986). Our measurements gave similar results. As pointed out by Spina & Smits (1986), cwever, the variation of convection velocity with distance from the wall makes these measurements difficult to interpret, and they appear to be of limited value. Using two wires placed a short distance apart to deduce structure angles is physically more meaningful.

(b) Conditionally Sampled Results

In our previous work, the primary basis for conditional sampling was the VITA technique, and it was applied to signals from a normal wire which measures mass-flow fluctuations $(\rho u)'$. The $(\rho u)'$ signal was converted to u' using the Strong Reynolds Analogy. The results obtained in zero pressure-gradient high-Reynolds number supersonic flows agreed well with similar results from subsonic, low Reynolds number flows. However, it is not at all clear what physical meaning can be attributed to the events detected by this technique. The interpretation is limited by the fact that VITA is a single point criterion, applied to measurements of a single component of the turbulent fluctuations. Our current emphasis, therefore, is to improve the detection technique to the point where the detected events can be given a more complete physical interpretation.

We have already found that the VITA technique can give a distorted picture of the flow structure. The primary technique which has allowed this critical interpretation of VITA is the development of a reliable and accurate crossed-wire probe, capable of giving signals proportional to instantaneous values of

u', v' (and u'v' , see Fernando, Donovan & Smits, 1987). The shear stress signal u'v' is highly intermittent, with sharp excursions from the background level (see Fig. 2). This signal is extremely suitable for conditional sampling. A simple threshold criterion was used to detect the events which make the greatest contribution to shear stress (threshold $= 2\ \overline{u'v'}$). These events are obviously of great practical interest. Quadrant analysis was used to classify the u'v' events into four categories: I (u+, v+), II (u-, v+), III (u-, v-), and IV (u+, v-).

The results were very revealing. Typically, the ensemble-averaged events were strong, and rather simple in shape (see Fig. 3). In particular, it should be noted that the u' event is single-sided, that is, it is either positive or negative. In contrast, when VITA was applied to the u' signal (instead of thresholding on u'v'), the event was doubled-sided, as shown in Fig. 4. These results suggest that VITA detection is subject to ambiguity, probably caused by the superposition of twc types of events which can only be separately identified by using quadrant analysis.

To explain the concept, consider two individual u events detected by the shear stress criteria, one lying in quadrant 2 and the other in quadrant 4 of the u-v plane. Both are single sided events. It is possible that VITA detects both these events as positive by checking the slope at their centers. The ensemble average of these two events would be a two sided event. Figure 5 clarifies the concept. Depending on exactly where the VITA technique checks the slope, thse events could have been picked up a negative events, giving a two sided negative event. This may explain why positive and negative VITA events are nearly mirror reflections of each other, about the velocity axis.

The quadrant analysis can be used to reveal another interesting result. The ensemble-averaged events in each quadrant (as shown, for example, in Fig. 3) plot trajectories in the u-v plane. Some examples of these loci are shown in Fig. 6. These trajectories will be compared to the results of the inviscid vortex skeleton model calculations described under Task C. The probability density of the shear stress in the u-v plane for the upstream boundary layer is plotted for various y/δ_o in Fig. 7. There is a definite change in the character of the probability density as y/δ_o increases. In the lower regions of the boundary layer all the equi-probability density contours are shaped more or less like ellipses, centered around the origin of the u-v plane, with the major axis lying in quadrants 2 and 4 at an angle to the u axis. As y/δ_o increases, the major axis rotates and aligns itself with the u axis. The centers of the equi-probability density contours show two different effects: the higher equi-probability contour centers move into quadrant 4, and the remaining contour centers move into quadrant 2. This behavior of the equi-probability contours with increasing y/δ_o does not change within the interaction. The contribution to the shear stress from each quadrant and the fractional residence time in each quadrant is shown in Figs. 8 and 9 respectively, for various x positions. It is seen that the trend in the fractional contribution to shear stress with y is the same at all stations. Lower in the boundary layer, contributions from quadrants 2 and 4 are approximately the same. Higher in the boundary layer the contribution from quadrant 2 is larger, even though the fractional residence time in quadrant 2 is smaller. This implies that the contributions to the shear stress from quadrant 2 consists of more intense shorter duration peaks in $u'v'$. This same conclusion

can be drawn from the "Hole Analysis" suggested by Lu and Willmarth (1970), and by examining the probability density of the time spent above a certain threshold shear stress, in quadrants 2 and 4. At all y/δ_0 there is a finite negative contribution to the shear stress from quadrants 1 and 3. Hence, the contributions from quadrants 2 and 4 add up to more than the total shear stress. As can be seen, in the outer part of the boundary layer, the contribution to the shear stress from quadrant 2 alone can be greater than the time-averaged shear stress.

c) <u>Conditionally-Sampled Flow Visualization</u>

We have continued to improve our flow visualization techniques. In particular, we are continuing to refine a method of conditionally sampling schlieren images of boundary layer structure in supersonic flow. In this technique, a hot-wire probe is used to detect the presence of strong, large-scale motions by using a real-time analog of the VITA detection method. Upon detection, a light source is flashed to record a microsecond exposure schlieren image on video tape. The hot-wire output is recorded simultaneously on the same video frame, and a typical image is shown in Fig. 10. The image was recorded using a CCD camera with linear gain so that the intensity can be linearly related to density gradient, and images can be added to get an ensemble-averaged picture. The conditionally sampled nature of the images means that we record only large events which are in the plane of the wire. We hope this method will remove the spatial integration effect of schlieren images. Preliminary results have been presented by Smith and Smits (1986).

We have recently purchased an image processing system, but unfortunately some minor hardware problems have been experienced. These problems have been fixed and the system has just been returned from the manufacturer. We hope to digitally enhance these images shortly and we expect that the processed images will be even clearer.

We have recently made high speed (40K frames/sec) laser schlieren movies of a supersonic boundary layer which clearly show the presence of strong large-scale motions convecting with the layer. Figure 11 is a typical sequence of alternate frames taken from one of these movies. (The camera exposes frames alternately on either side of the film.) Although it is possible to "threshold" the schlieren images so that only the very strongest structures are detected, the spatial integration inherent in the schlieren technique makes it difficult to produce convincing images of individual structures.

One way around this may be to photograph laser sheet cross-sections through smoke or some other light scattering medium introduced at some strategic point in the flow. Unfortunately, a conventional continuous laser (e.g. 5 watt He-Ne) does not have nearly enough power for short-time (e.g. $1\mu s$) exposure of movie film (or still photographs) from light scattered from particles. A high intensity flashed laser light source is required.

We are awaiting approval of the Supplement to AFOSR Grant 85-0126 dated December 31, 1986, to purchase a Plasma Kinetics copper vapor laser to provide this light source. The particular laser requested has an average power output of 10 watt, with a repetition rate of 10 kHz, and a pulse width of 14 nanosec. This light source will make it possible to obtain high contrast, freeze-frame pictures of supersonic flow structure at realistic data rates.

(d) Future work

Work is continuing on the search for new and improved conditional sampling techniques. A six-wire probe is being developed to provide information in the spanwise and normal directions simultaneously. We are awaiting permission to reallocate $19,600 in Contract F49620-86-C-0094 from salaries to the equipment category in order to purchase the necessary hot-wire instrumentation. Also included in the reallocation request is the optics for laser scanning which will improve our flow visualization capabilities. We hope to construct the first image-processed pictures of boundary layer structures.

TASK B: LONGITUDINAL CURVATURE EFFECTS IN TURBULENT BOUNDARY LAYERS

This task is an experimental investigation of the distortion and relaxation of an initially self-preserving zero-pressure gradient subsonic turbulent boundary layer (Re_θ = 5700) subjected to 90° of strong convex curvature (δ_o/R = 0.07). The study provides subsonic zero-pressure gradient layer measurements (i.e. upstream of the curvature) which can be used for direct comparison with the corresponding measurements in the supersonic flow. Also, it allows us to study the behavior of structural parameters subsequent to the severe distortion imposed by the convex curvature.

In the earlier work of Alving and Smits (1986), mean flow measurements were used to investigate the influence of two different pressure distributions in the region of curvature. In the first case, the two walls were concentric so that the boundary layer on the convex wall was subjected to a strong acceleration and deceleration within the bend. In the second case the effects of pressure gradient were minimized by contouring the outer wall. Suction was

applied in the region of the expansion of the outer wall to prevent the boundary layer from separating in the adverse pressure gradient (see Fig. 12).

For both cases the distorted boundary layer experienced several stages of recovery on the flat plate downstream. In the first stage of recovery, of length around $25\delta_o$, the effects of different pressure gradient histories within the bend were found to be significant. However, further downstream, in the second stage of recovery only the long-lasting effects of curvature remained. Although the rate of recovery slows down, Alving and Smits found that the boundary layer appeared to overshoot the flat plate zero pressure gradient state.

In the concentric wall case the outer wall boundary layer was greatly thickened and began to interfere with the test wall boundary layer at a point approximately $30\delta_o$ downstream of the end of curvature. Consequently this case has not been studied further.

The contoured wall case has been subjected to further refinement. In particular, the strength of the suction has been carefully tuned so that the thickness of the outer wall boundary layer is minimized at the exit of the bend. This provides the greatest usable length of the test section without contamination of the test wall boundary layer. More uniformity was also observed in the spanwise skin friction distribution (see Fig. 13) indicating a substantially two-dimensional boundary layer.

A complete set of Reynolds stress measurements were presented by Alving, Watmuff and Smits (1987). The dynamic calibration technique was adopted for the crossed-wire probe so as to accurately monitor the development of the internal equilibrium layer. The advantage of this method is that the sensi-

tivities to both velocity components are determined directly without the need to measure wire angles or assume heat transfer laws. The method is based on that used by Watmuff et al. (1983) but now offers several improvements including reduced calibration running time.

The turbulence results display a spectacular recovery behavior, see Figs. 14(a)-(d). As observed by Smits et al. (1979) the shear stress in the outer part of the layer falls to very low values, whereas in the inner region a peak appears which then progresses out from the wall further downstream. At the furthest downstream stations, the rate of relaxation of all turbulence quantities becomes very slow, and their behavior is very similar. Except for the first station in the recovery region, the behavior of $\overline{u'^2}$, $\overline{v'^2}$ and $\overline{w'^2}$ follow that shown by the shear stress. Hence, it is not surprising that the structure parameter $a_1 = -\overline{u'v'}/q^2$ relaxes quickly and within $25\,\delta_0$ downstream of the bend the profile of a_1 is almost identical to that observed upstream of the bend. In contrast, the absolute stress levels relax slowly. For example, at the furthest downstream station, the inner half of the layer has virtually constant shear stress, and this observation is consistent with the larger extent of the logarithmic variation in the mean velocity profile here. It is clear that the relaxation process is far from complete, even at locations greater than $90\,\delta_0$ from the exit of the bend. Thus convex curvature, which is considered a stabilizing perturbation, causes strongly increased mixing for large distances downstream after the end of curvature. This seemingly contradictory result is similar to the recovery from strong concave (destabilizing) curvature observed by Smits et al. (1979) in which high stress levels at the exit from curvature were quickly reduced below the upstream level.

In response to the evolving nature of this research task, and in collaboration with the contract monitor, we have developed a new focus for Task B. Instead of concentrating on Reynolds stress measurements for a range of curvature parameters, we have decided that it is more profitable to focus on the measurement of structural parameters. This approach will allow a better understanding of curvature effects, and also provide a direct comparison with the supersonic boundary layer results.

Structure angles have been derived from the space-time correlation of signals from two normal wires (i.e. the technique of Spina and Smits 1986). The results for the upstream boundary layer (see Fig. 15) show that the angle lies between 40 and 50 degrees for $y/\delta_0 < 0.5$. However, the angle increases further from the wall and reaches a value around $60°$ near the edge of the layer. There appears to be a consistent increase in θ far downstream which may be related to the new equilibrium state observed in the Reynolds stress profiles. This may imply that several different types of events may be contributing to the space-time correlation, and that some type of conditional sampling will probably be necessary to sort out the influence of the various types of events. Work is continuing in this area.

TASK C: ANALYSIS AND CONTROL OF WALL-BOUNDED VORTEX LOOPS

It is generally accepted that the structure of turbulent boundary layers can be described in terms of "hairpin" or "lambda"-shaped vortex loops. This physical model seems to describe equally well the dynamics of small- and large-scale motions (see, for example, Head & Bandyophadyay, 1981, Perry and Chong, 1982, and Smith, 1984). The interpretation of our conditionally-sampled

measurements has been strongly influenced by the hairpin loop model, and to aid this interpretation further we have begun to investigate the behavior of simple wall-bounded vortex loops.

The loops are generated by a a lambda-shaped wire which periodically forces laminar, vortical fluid away from the wall (see Fig. 16). By controlling their formation, interactions among multiple vortex loops can be studied. The experiments are being conducted in a large low-speed smoke tunnel so that simultaneous flow-visualization and hot-wire measurements are possible.

The nature of the single loops is illustrated in Figs. 17 and 18. Figure 17 shows a plan view of the loop, indicating the characteristic splaying of the legs of the vortex, and the omega-shaped head. Figure 18 shows a side view, together with signals proportional to u' and v', as measured by the hot-wire probe visible on the left. The signals are similar to the ensemble-averaged, second-quadrant u' and v' signals shown in Fig. 3.

Simple analytical models have been developed to model these experimental vortex loops using straight-line vortex filaments. The example given in Fig. 19 shows a simple line array of five loops, and the u' and v' signals corresponding to two positions are shown in Fig. 20. The similarities to the ensemble-averaged, second- and fourth-quadrant u' and v' signals shown in Fig. 3 are obvious. The loci on the (u', v') plane for different observers are shown in Fig. 21, and there are some interesting comparisons possible with the results shown in Fig. 5.

We will continue to use the vortex loop study as support for the interpretation of our conditionally sampled measurements. We will begin with the study of interacting loops. We have already performed some preliminary work to

examine vortex pairing by generating two different strength vortex loops down the center of the tunnel. This work was presented by Donovan et al. (1986).

Impact of A. J. Smits Sabbatical: From February 17, 1987 to August 15, 1987, the principal investigator, A. J. Smits, will be on sabbatical at the Institut Mecanique Statistique de la Turbulence at Marseille, France.

References

Acarlar, M. S. and Smith, C. R. (1984), "An Experimental Study of Hairpin-Type Vortices as a Potential Flow Structure of Turbulent Boundary Layers," Report FM-5, Dept. of Mech. Engrg. and Mechanics, Lehigh University.

Alving, A. E. and Smits, A. J. (1986), "The Recovery of a Turbulent Boundary Layer from Longitudinal Curvature," AIAA Paper 86-0435, AIAA 24th Aerospace Sciences Meeting, Reno, Nevada, January.

Alving, A. E., Watmuff, J. H. and Smits, A. J. (1987), "The Relaxation of a Turbulent Boundary Layer Far Downstream of a Short Region of Convex Curvature," AIAA Paper 87-0196, AIAA 25th Aerospace Sciences Meeting, Reno, Nevada, January.

Brown, G. L., Thomas, A. S. W. (1977), "Large Structure in a Turbulent Boundary Layer," Phys. Fluids, Vol. 20.

Donovan, J., Fernando, E. M., Spina, E. F., Watmuff, J. H. and Smits, A. J. (1986), "Active Control of Wall-Bounded Vortex Loops," Presented at the Thirtyninth Annual Meeting of the American Physical Society, Columbus, Ohio, November.

Fernando, E. M. and Smits, A. J. (1987) "The Effects of Adverse Pressure Gradient on the Behavior of a Supersonic Turbulent Boundary Layer," AIAA Paper 87-1286, AIAA 19th Fluid Dynamics, Plasma Dynamics & Laser Conference, Honolulu, Hawaii, June.

Fernando, E.M., Donovan, J. and Smits, A. J. (1987), "The Calibration and Operation of a Constant-Temperature Crossed-Wire Probe in Supersonic Flow," to be presented at ASME Fluids Engineering Division Spring Meeting, June.

Head, M. R. and Bandyopadhyay, P. (1981), "New Aspects of Turbulent Boundary Layer Structure," Journal of Fluid Mechanics, Vol. 107, p. 297.

Lu, S. S. and Willmarth, W. W. (1970), "Measurements of the Structure of the Reynold Stress in a Turbulent Boundary Layer," Journal of Fluid Mechanics, Vol. 60, pp. 481-511.

Perry, A. E., Chong, M. S. and Lim, T. T., "The Vortex Shedding Process Behind Two-Dimensional Bluff Bodies," Journal of Fluid Mechanics, Vol. 116, p. 77.

Robinson, S. K. (1986), "Space Time Correlation Measurements for a Compressible Turbulent Boundary Layer," AIAA Paper 86-1130, AIAA/ASME 4th Fluid Mechanics, Plasma Dynamics and Lasers Conference, Atlanta, Georgia, May.

Smith, C. R. (1984), "A Synthesized Model of the Near-Wall Behavior in Turbulent Behavior in Turbulent Boundary Layers," Proceedings of Eighth Symposium on Turbulence, (Ed. G. K. Patterson and J. L. Zakin), Department of Chemical Engineering, University of Missouri-Rolla.

Spina, E.F. and Smits, A.J. (1986), "Organized Structures in a Supersonic Turbulent Boundary Layer," to be presented, Ninth Australasian Fluid Mechanics Conf., Univ. of Auckland, New Zealand, December.

Watmuff, J. H., Perry, A. E. & Chong, M. S. (1983), "A Flying Hot-Wire System," Experiments in Fluids, Vol. 1, pp. 63-71.

Appendix B

Publications Produced Under
Sponsorship of
AFOSR Grant 85-0126

A. Published Papers

1. Baskaran, V., Smits, A.J. and Joubert, P.N., "A Turbulent Flow over a Curved Hill. Part I. Growth of an Internal Boundary Layer", submitted for publication, Journal of Fluid Mechanics, 1986.

2. Smits, A.J. and Muck, K.C., "Experimental Study of Three Shock-Wave/Turbulent Boundary-Layer Interactions", submitted for publication, Journal of Fluid Mechanics, 1986.

3. Fernholz, H.H., Smits, A.J. and Dussauge, J.-P., (Eds.), "A Survey of Measurements and Measuring Techniques in Rapidly Distorted Compressible Turbulent Boundary Layers," NATO-Advisory Group for Aerospace Research and Development AGARDograph, under preparation.

4. Smits, A.J. and Bogdonoff, S.M., "A 'Preview' of Three-Dimensional Shock-Wave/Turbulent Boundary Layer Interactions," presented at the IUTAM Symposium on Turbulent Shear Layer/Shock Wave Interactions, Palaiseau, France, September 9-12, 1985. Published by Springer Verlag, 1986.

5. Dussauge, J.-P., Muck, K.C. & Andreopoulos, J. "Properties of wall pressure fluctuations in a separated flow over a compression ramp", IUTAM Symp. on Turbulent Shear Layer/Shock Wave Interactions, Palaiseau, France, Sept. 1985. Published Springer-Verlag, 1986.

6. Spina, E.F. and Smits, A.J., "Organized Structures in a Compressible Turbulent Boundary Layer", accepted for publication, Journal of Fluid Mechanics, 1986.

7. Andreopoulos, J. & Muck K.C., "Some new aspects of shock wave boundary layer interactions in compression ramp flows", submitted for publication, Journal of Fluid Mechanics.

8. Muck, K.C, Andreopoulos, J. & Dussauge, J.-P, "The structure of a separated flow over a two-dimensional compression ramp" (under preparation)

B. Papers published in Conference Proceedings

1. Alving, A.E. and Smits, A.J., "The Recovery of a Turbulent Boundary Layer from Longitudinal Curvature," AIAA Paper 86-0435, AIAA 24th Aerospace Sciences Meeting, Reno, Nevada, January 1986.

2. Andreopoulos, J. & Muck, K.C., "Some new aspects of shock wave boundary layer interactions in compression ramp flows", AIAA Paper #86-0342, AIAA 24th Aerospace Sciences Meeting, Reno, Nevada, January 1986.

3. Alving, A.E., Watmuff, J.H. and Smits, A.J., "The Relaxation of a Turbulent Boundary Layer Far Downstream of a Short Region of Convex Curvature", AIAA Paper 87-0196, AIAA 25th Aerospace Sciences Meeting, Reno, Nevada, January 1987.

4. Selig, M.S., Andreopoulos, J., Muck, K.C., Dussauge, J.P. and Smits, A.J., "Simultaneous Wall-Pressure and Mass-Flow Measurements Downstream of a Shock Wave/Turbulent Boundary Layer Interaction," AIAA Paper 87-0550, AIAA 25th Aerospace Sciences Meeting, Reno, Nevada, January 1987.

5. Spina, E.F. and Smits, A.J., "The Effect of Compressibility on the Large-Scale Structure of a Turbulent Boundary Layer", AIAA Paper 87-0145, AIAA 25th Aerospace Sciences Meeting, Reno, Nevada, January 1987.

6. Spina, E.F. and Smits, A.J., "Organized Structures in a Supersonic, Turbulent Boundary Layer", Presented at Ninth Australasian Fluid Mechanics Conference, Univ. of Auckland, Auckland, N.Z., December 1986.

7. Watmuff, J. H., "Wind Tunnel Contraction Design," Presented at the Ninth Australasian Fluid Mechanics Conference, Auckland, New Zealand, December 1986.

8. Fernando, E.M. and Smits, A.J., "The Effects of an Adverse Pressure Gradient on the Behavior of a Supersonic Turbulent Boundary Layer", to be presented at AIAA 19th Fluid Dynamics, Plasma Dynamics and Laser Conference, Honolulu, Hawaii, September 1986.

9. Fernando, E. M., Spina, E. F., Donovan, J. F., and Smits, A. J., "Detection of Large-Scale Organized Motions in a Turbulent Boundary Layer." Paper accepted for Sixth Symposium on Turbulent Shear Flows, Toulouse, France, 1987.

C. Reports & Conference Papers

1. Rong, B.S., Tan, D.K.M. and Smits, A.J., "Calibration of the Constant-Temperature Normal Hot-Wire Anemometer in Transonic Flow", Princeton University, Dept. of Mechanical and Aerospace Engineering, Report #1696, 1985.

2. Rong, B.S., Tan, D.K.M. and Smits, A.J., "Calibration of the Constant-Temperature Inclined Hot-Wire Anemometer in Transonic Flow", Princeton University, Dept. of Mechanical and Aerospace Engineering, Report #1698, 1985.

3. Alving, A.E. and Smits, A.J., "Drag Reducing Aspects of Surface Curvature", presented at the Drag Reduction and Boundary Layer Control Symposium, Washington, D.C., Oct. 1985.

4. Spina, E.F. and Smits, A.J., "Organized Structure in a Sup ersonic Turbulent Boundary Layer," Paper #CP1, 38th Annual Meeting, Division of Fluid Dynamics, Bulletin of the American Physical Society, Nov. 1985.

5. Spina, E.F. and Smits, A.J., "Organized Structures in a Supersonic Turbulent Boundary Layer", Princeton University, Dept. of Mechanical and Aerospace Engineering, Report #1736, 1986.

6. Fernando, E.M. and Smits, A.J., "A Data Compilation for a Supersonic Turbulent Boundary Layer Under Conditions of an Adverse Pressure Gradient", Princeton University, Dept. of Mechanical and Aerospace Engineering, Report #1746, 1986.

7. Smith, M. and Smits, A. J., "Conditionally-Averaged Schlieren Video Images of Large-Scale Motions in Supersonic Turbulent Boundary Layers," Presented at the 39th Annual Meeting, Division of Fluid Dynamics, American Physical Society, Columbus, Ohio, November 1986.

8. Donovan, J., Fernando, E. M., Selig, M. S., Spina, E. F., Watmuff, J. H. and Smits, A. J., "Active Control of Wall-Bounded Vortex Loops," Presented at the 39th Annual Meeting, Division of Fluid Dynamics, American Physical Society, Columbus, Ohio, November 1986.
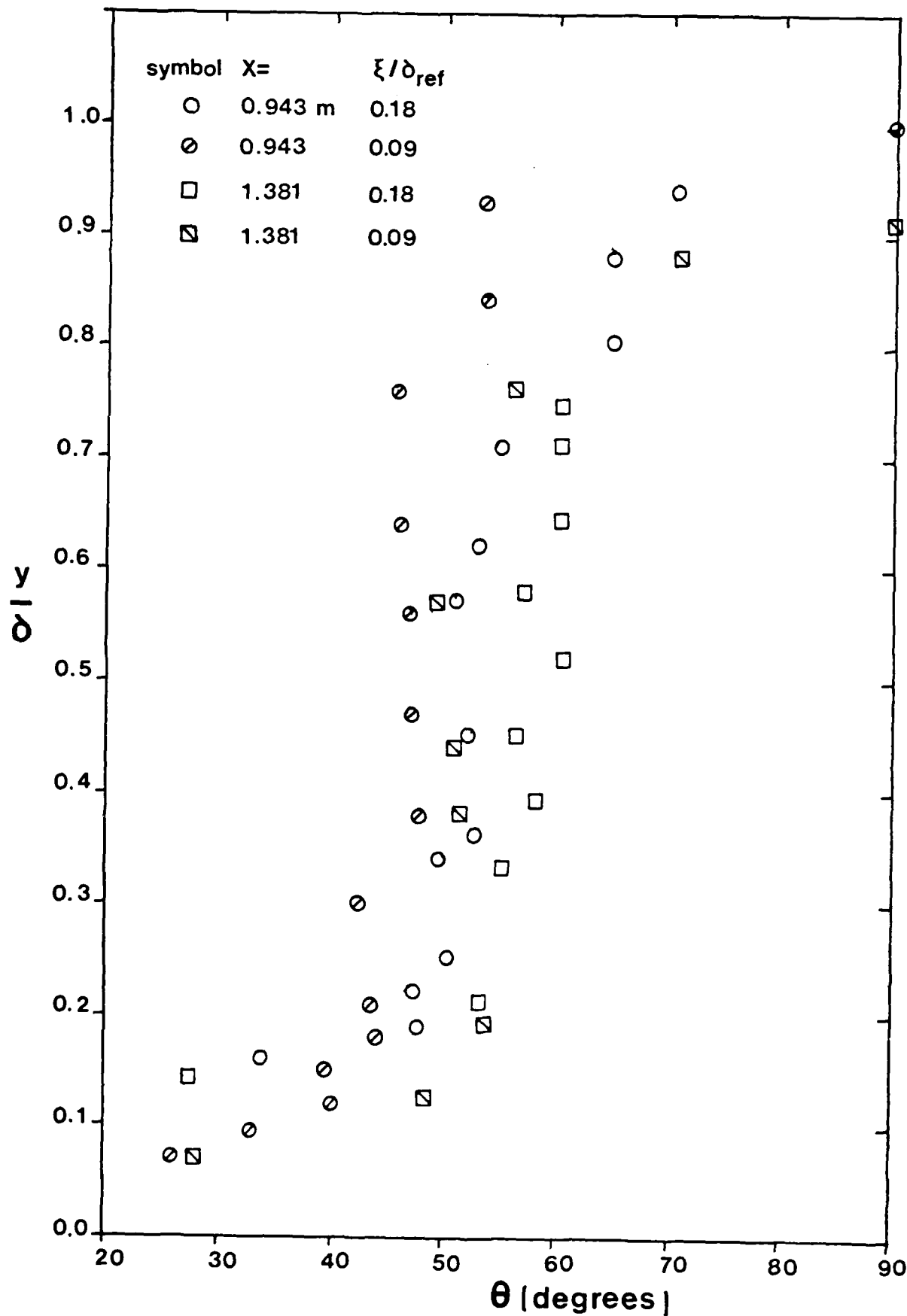
Fig. 1. Structure angle deduced from space-time correlation measurements in
an adverse pressure gradient supersonic boundary layer.
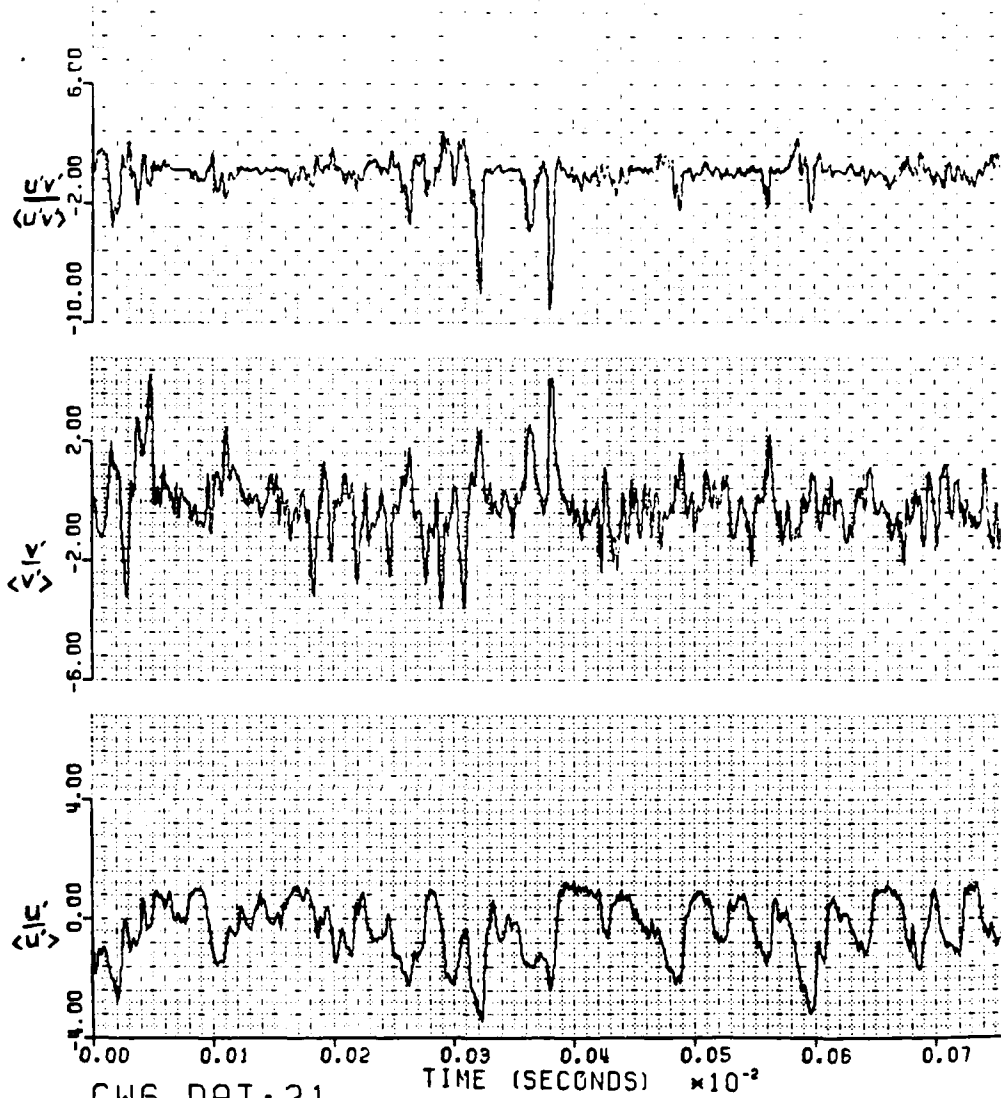
CW6.DAT;21
LONG TIME MEAN SUBTRACTED FROM DATA & DATA NORMALIZED BY RMS OF SIGNAL
4096 POINTS FROM THE 2 TH. WRITTEN RECORD. OF THE 1TH. SAMPLED RECORD.

Fig. 2. Signals of u'v', v' and u' deduced from the output of a crossed-wire in zero pressure gradient supersonic boundary layer at $y/\delta = 0.65$.
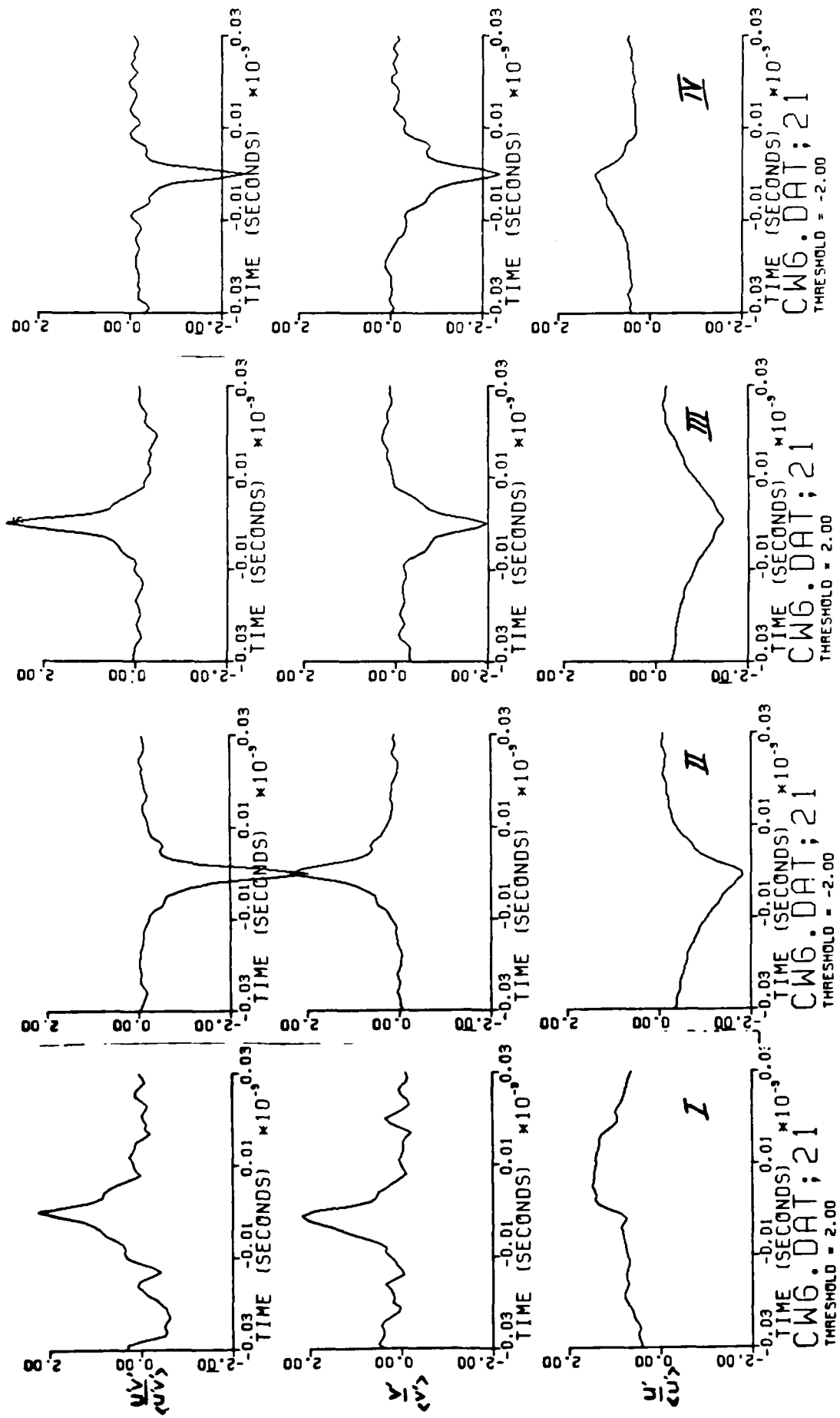
Fig. 3. Ensemble-averaged events based on threshold detection applied to u'v' signal at y/δ = 0.65: Quadrants I (u+, v+); II (u−, v+); III (u−, v−); IV (u+, v−)
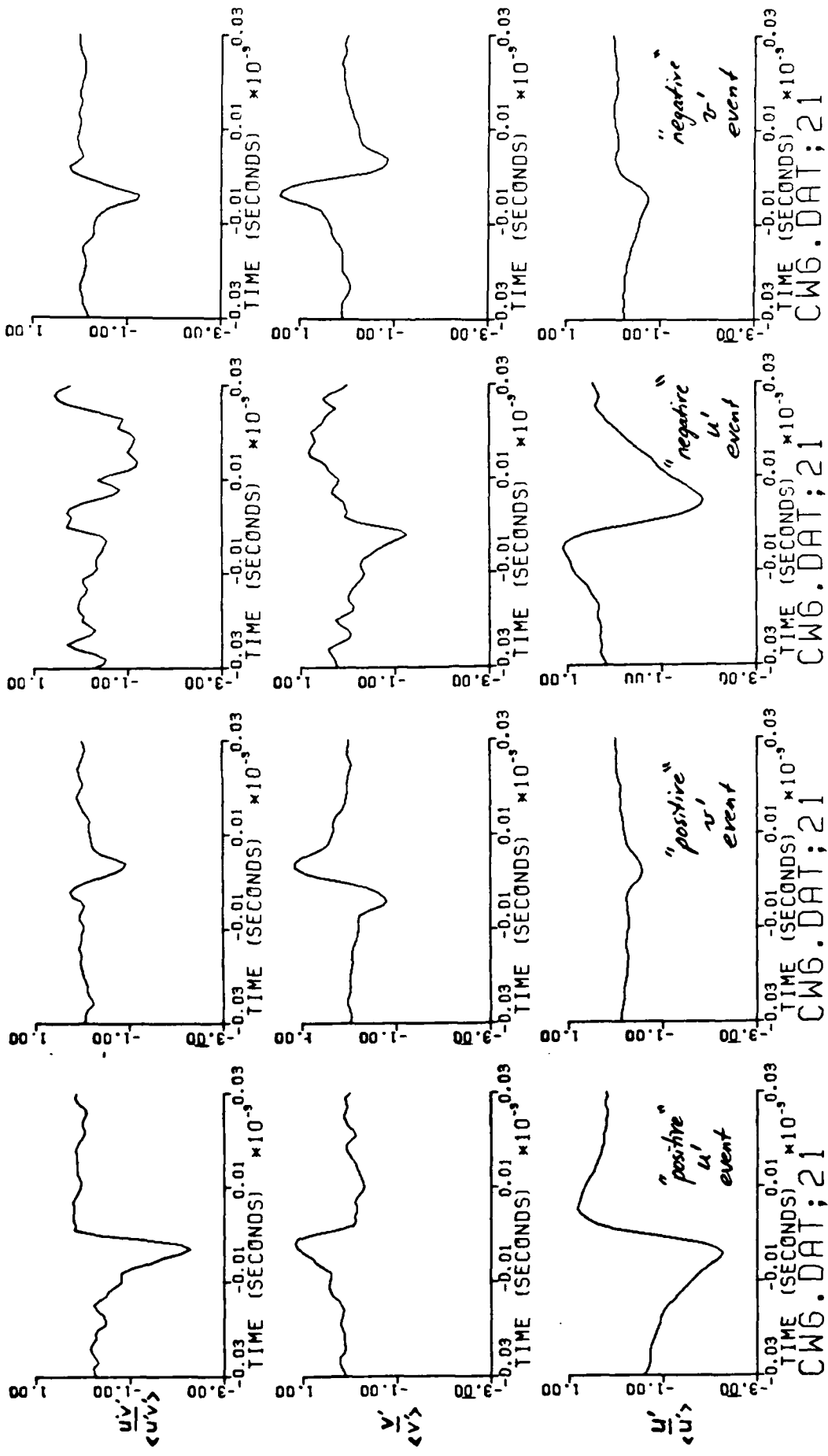
Fig. 4. Ensemble-averaged event based on VITA at $y/\delta = 0.65$.
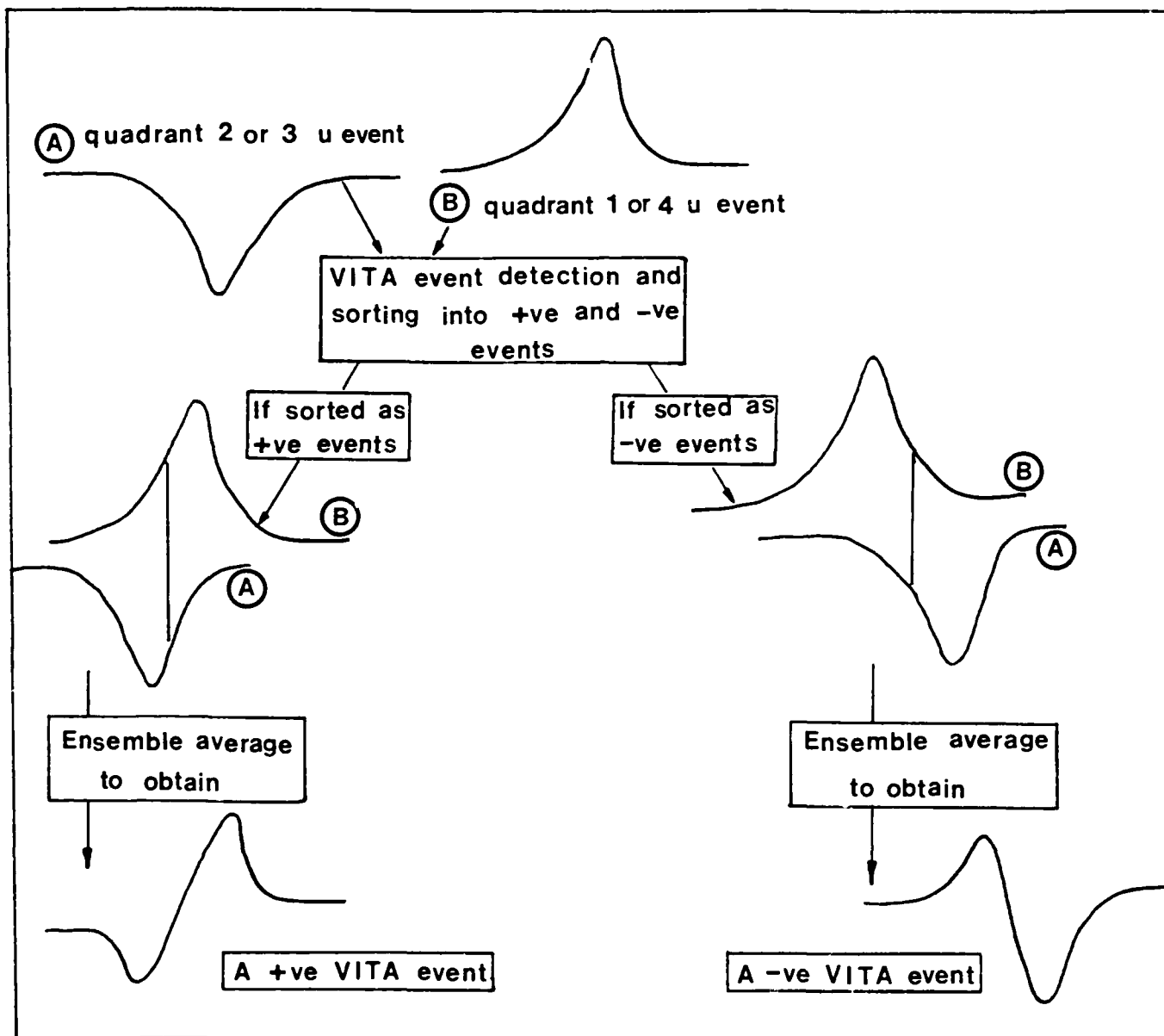
Fig. 5. A possible explanation as to the difference between ensemble averages obtained by the VITA technique and by threshold criteria applied to the shear stress.
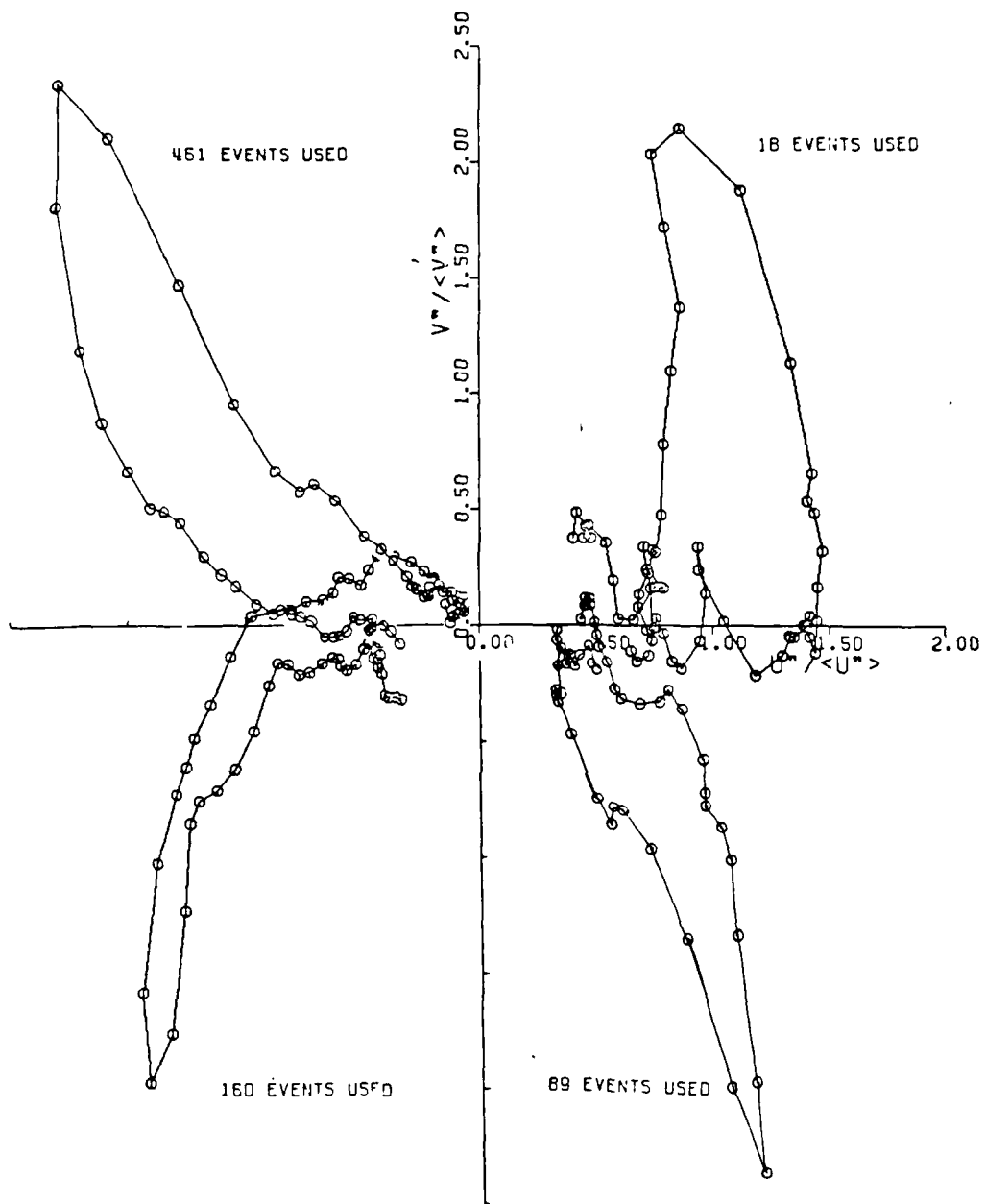
Fig. 6. Loci of the ensemble-averaged events shown in Fig. 3 in the (u', v') plane.

Note that $\langle u' \rangle = 18\, m/s$, $\langle v \rangle = 13.8\, m/s$
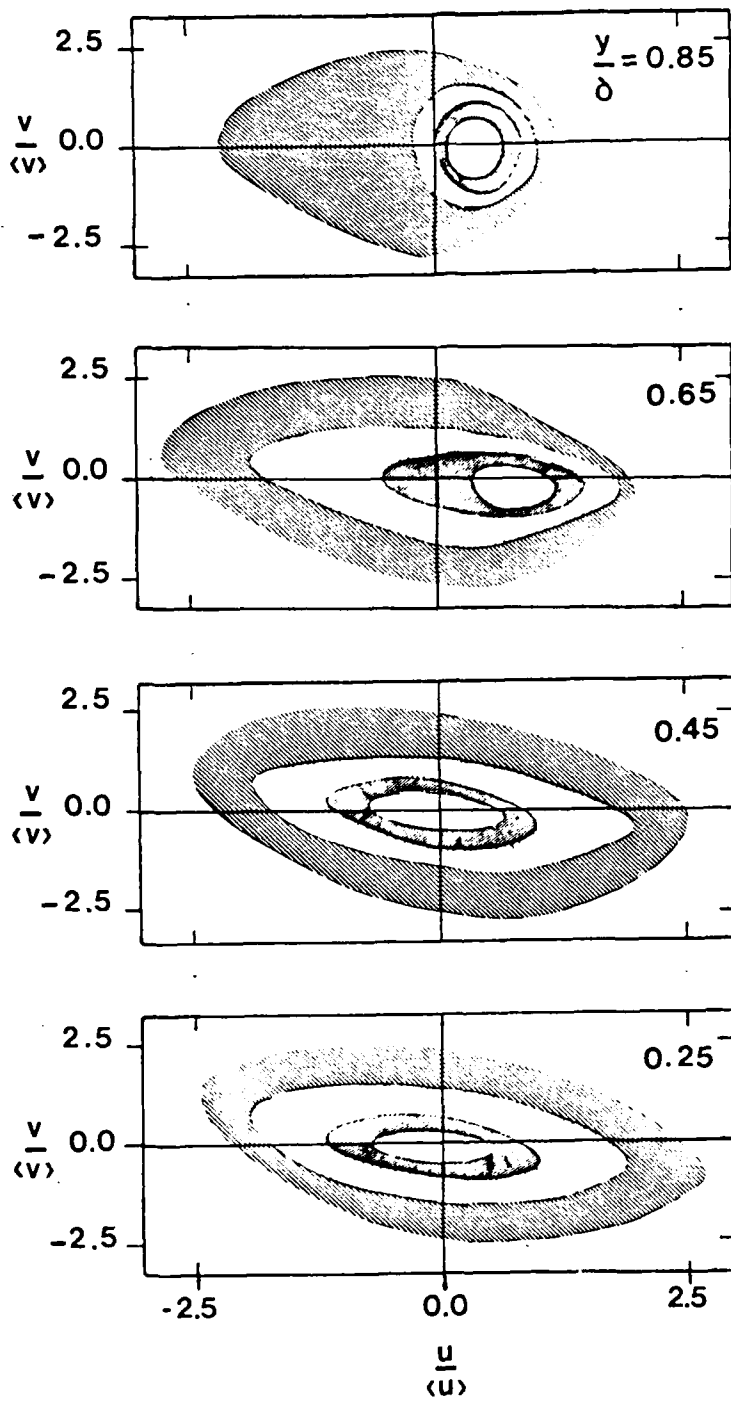
Fig. 7. Variation with wall distance of equi-probability contours of u'v' in the u-v plane for a zero pressure gradient turbulent boundary layer.
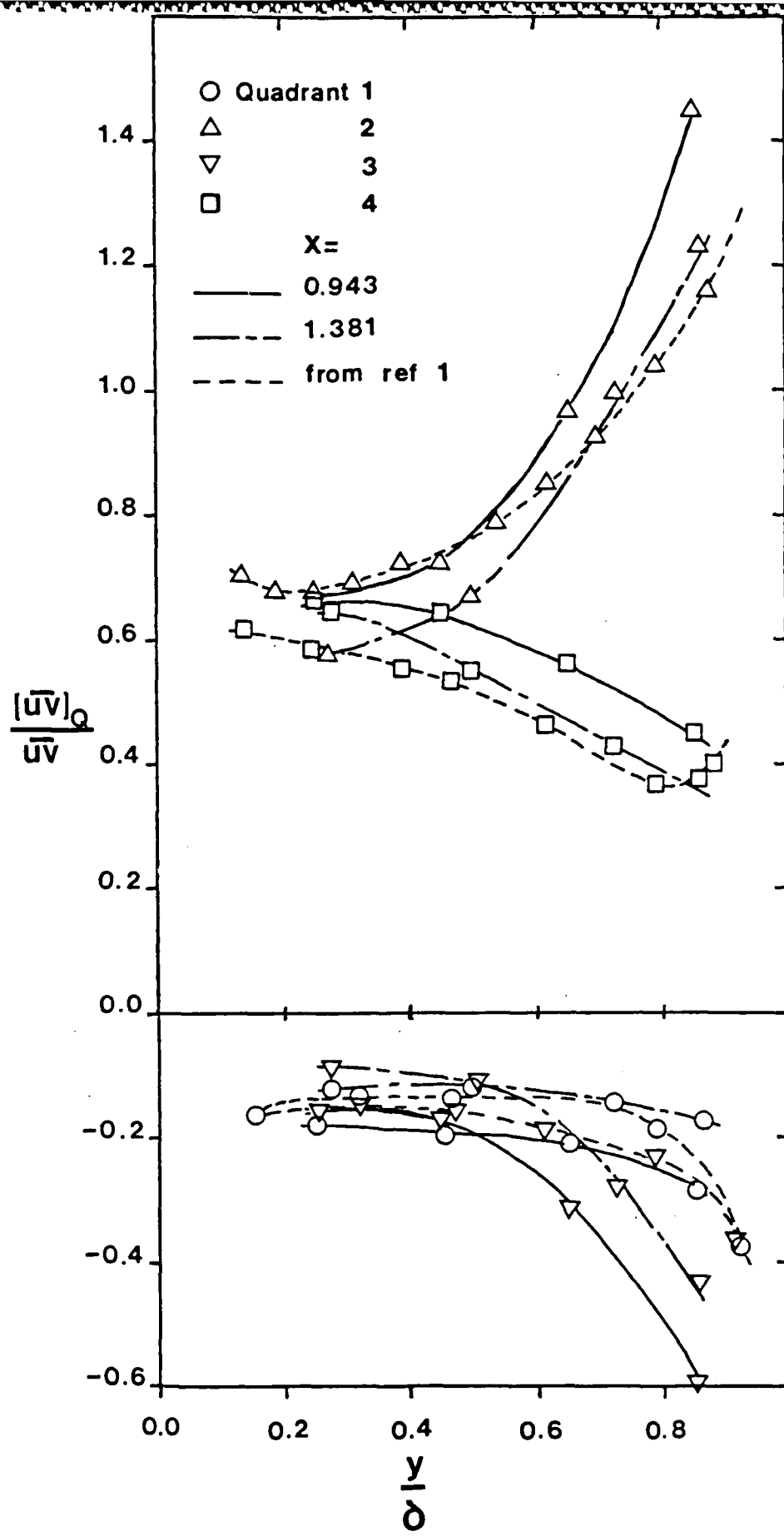
Fig. 8. Contribution to the shear stress from each quadrant of the u-v plane.
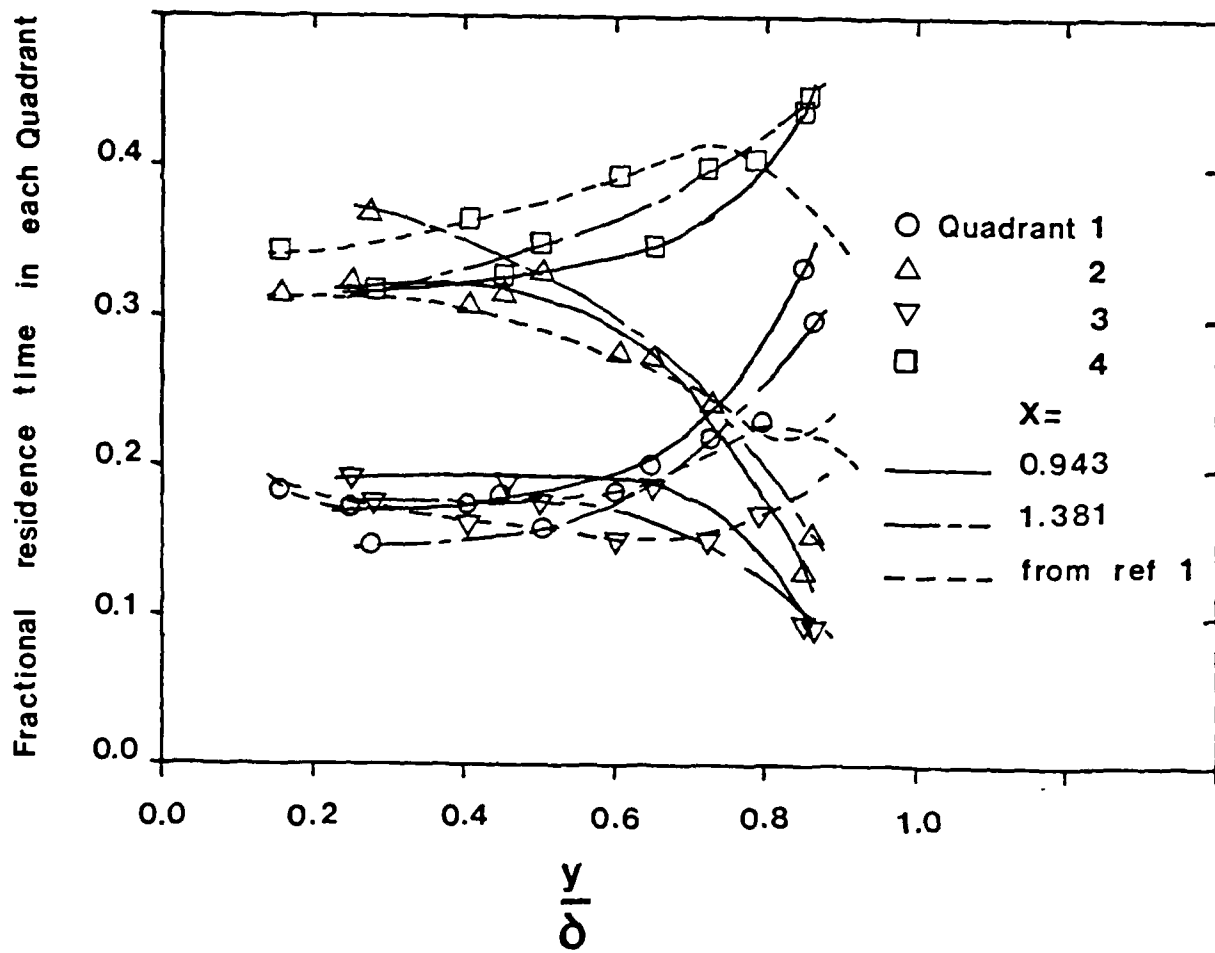
Fig. 9. Fractional residence time in each quadrant of the u-v plane.
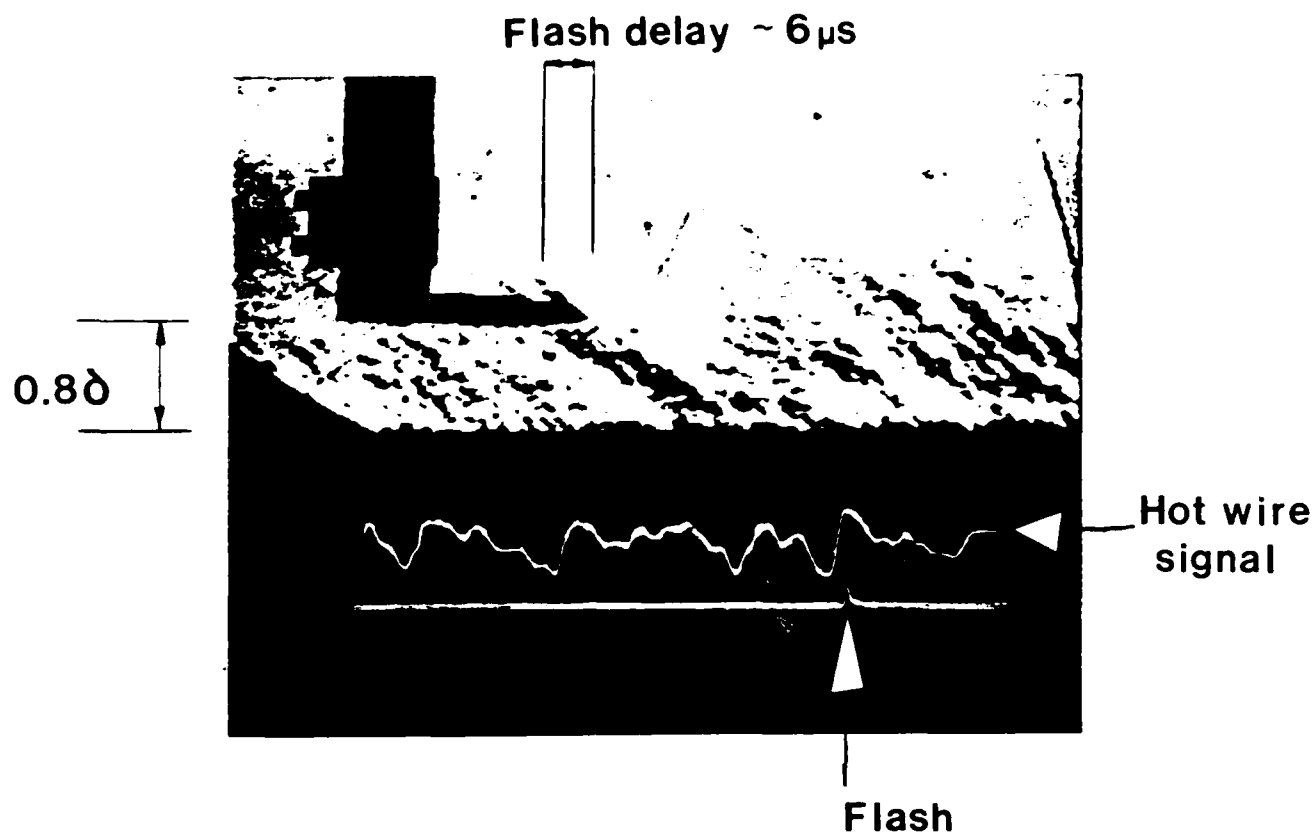
Fig. 10. Microsecond schlieren video image of zero pressure gradient supersonic boundary layer. The hot-wire probe is on the left, and the corresponding signal is shown near the bottom of the picture. The time scale corresponds approximately to the length scale of the picture.

$t = 300\mu s$

$t = 250\mu s$

$t = 200\mu s$

$t = 150\mu s$

$t = 100\mu s$

$t = 50\mu s$

$t = 0.0$
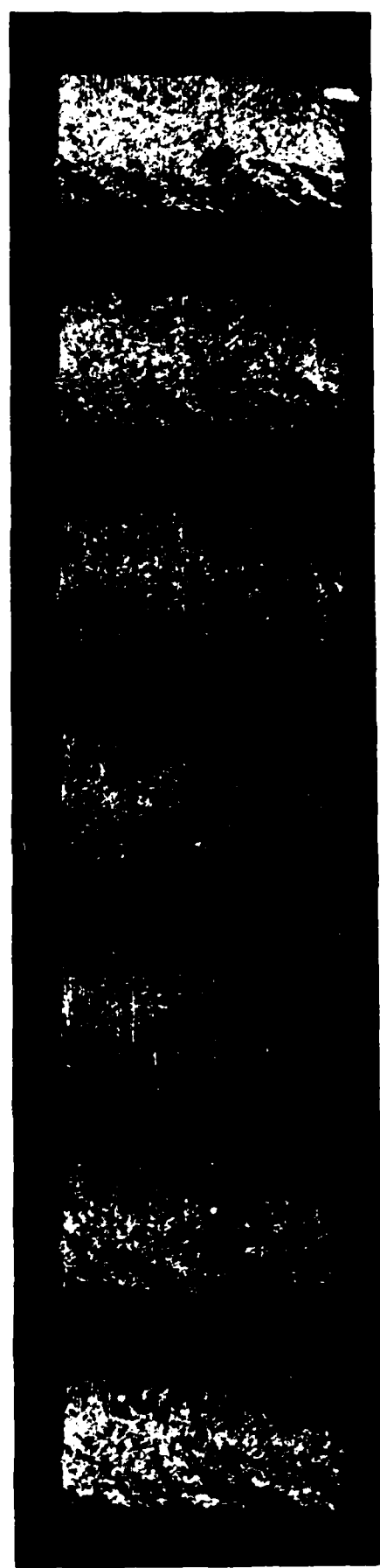
Time

Fig. 11.   Alternate frames from a 40K frame/sec laser schlieren movie of a
supersonic turbulent boundary layer.   Note convection of large-scale
motions from right-to-left.
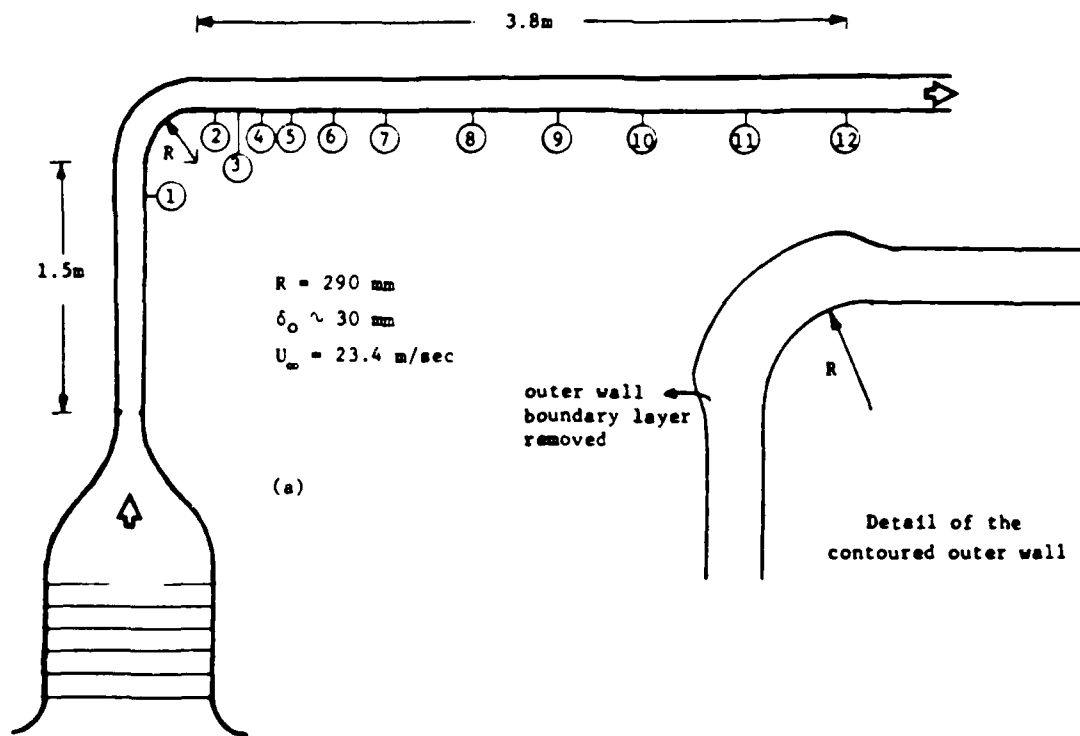
Fig. 12. Schematic of subsonic curved wall experiment, showing detail of the contoured outer wall.
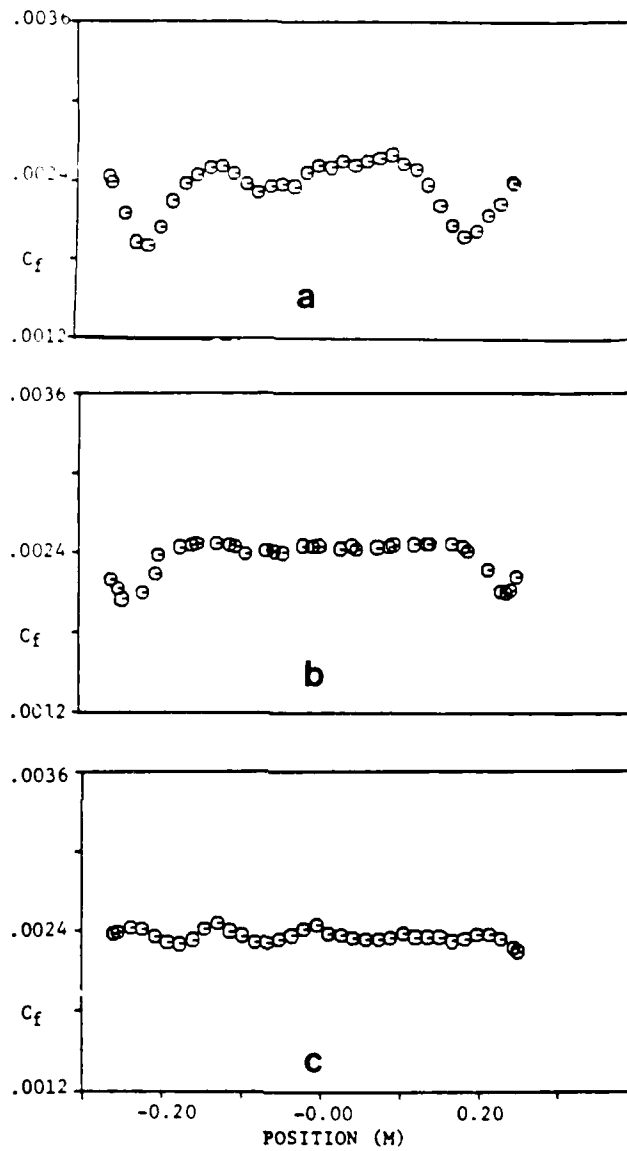
Fig. 13. Spanwise skin friction variation. Measurementws taken at s = 3.00 m (a) previous results with no sidewall boundary layer control, (b) previous results with sidewall jets within bend, (c) present results, with sidewall jets.
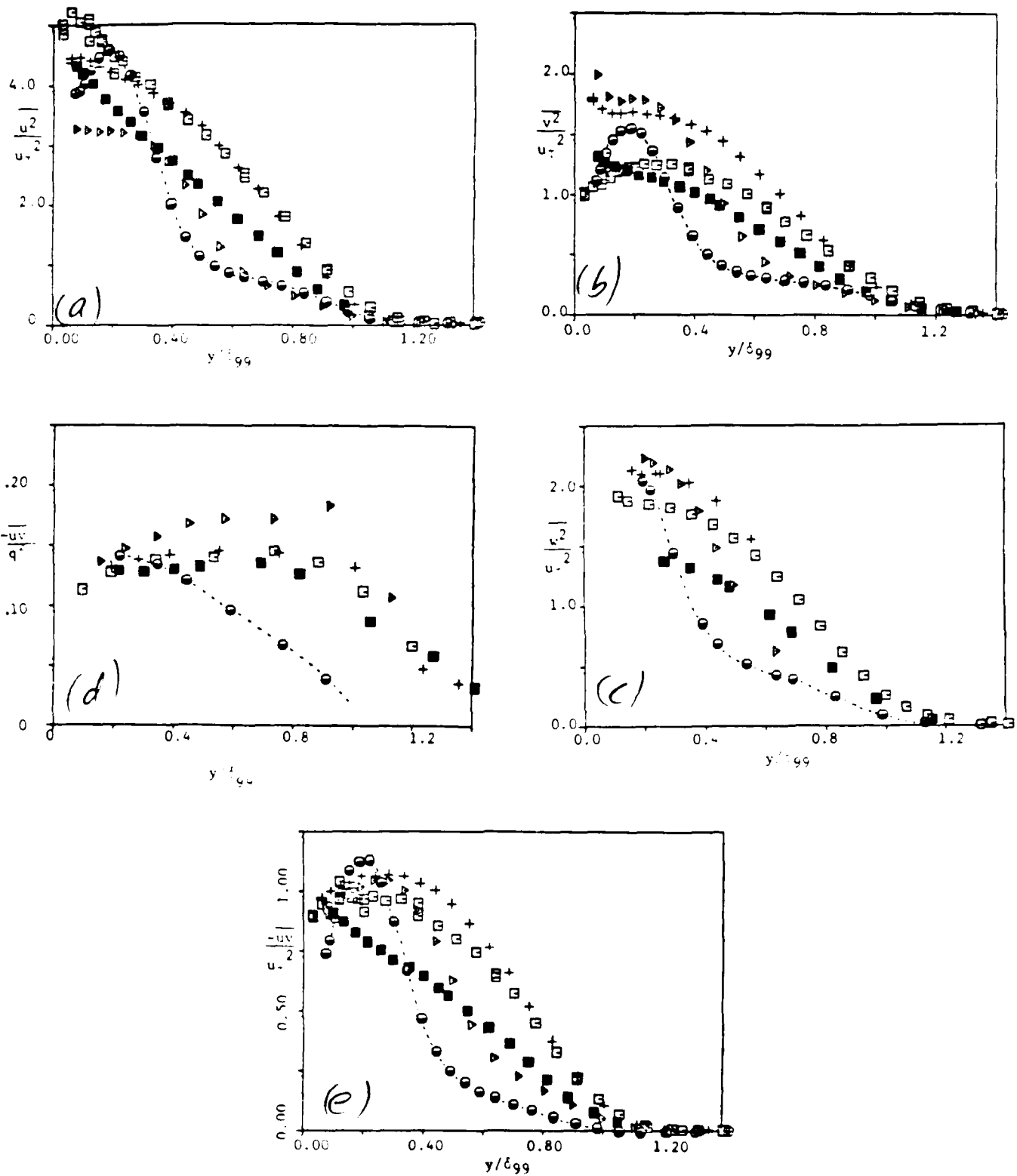
Fig. 14. Upstream profile and relaxation downstream of convex curvature of
(a) $\overline{u'^2}/U_\tau^2$, (b) $\overline{v'^2}/U_\tau^2$, (c) $\overline{w'^2}/U_\tau^2$, (d) $-\overline{u'v'}/U_\tau^2$,
(e) Structure parameter $-\overline{u'v'}/q^2$

Key: ■ station 1 ; ● station 3 ;
      ▷ station 5 ; + station 7 ;
      □ station 9 .
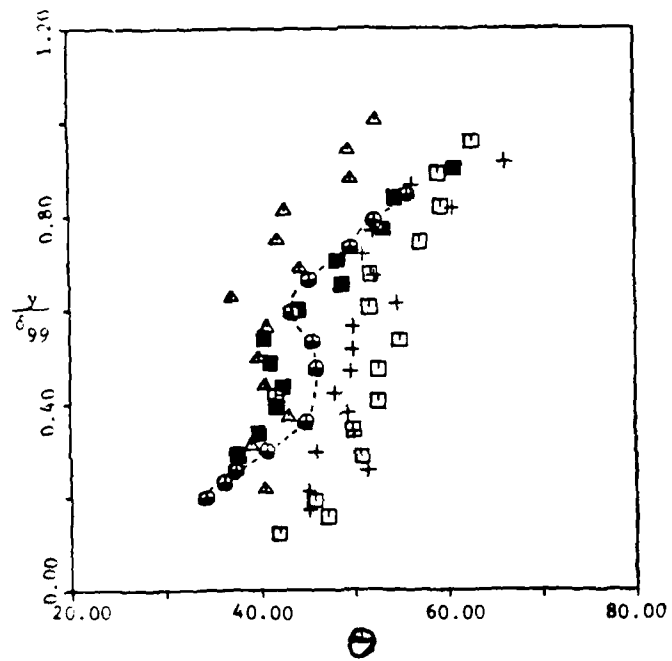
Fig. 15. Streamwise development of structure angle. Symbols as in Fig. 14.
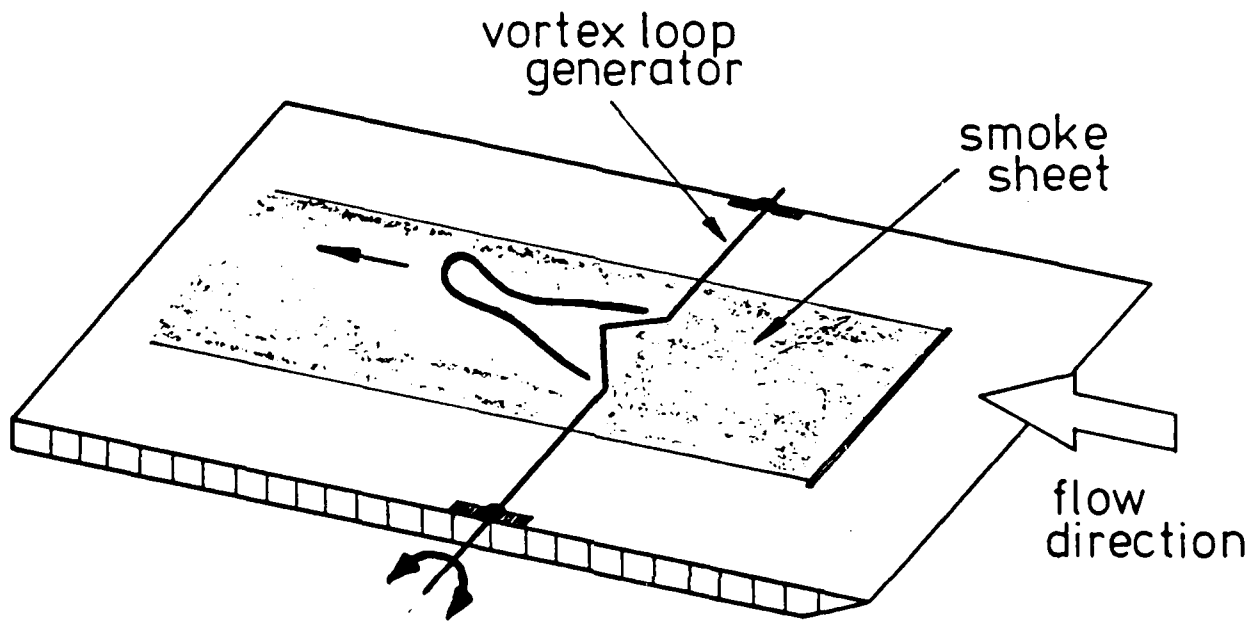
Fig. 16. Vortex loop generator.

Fig. 17. Plan view of single loop. Flow is from right to left.
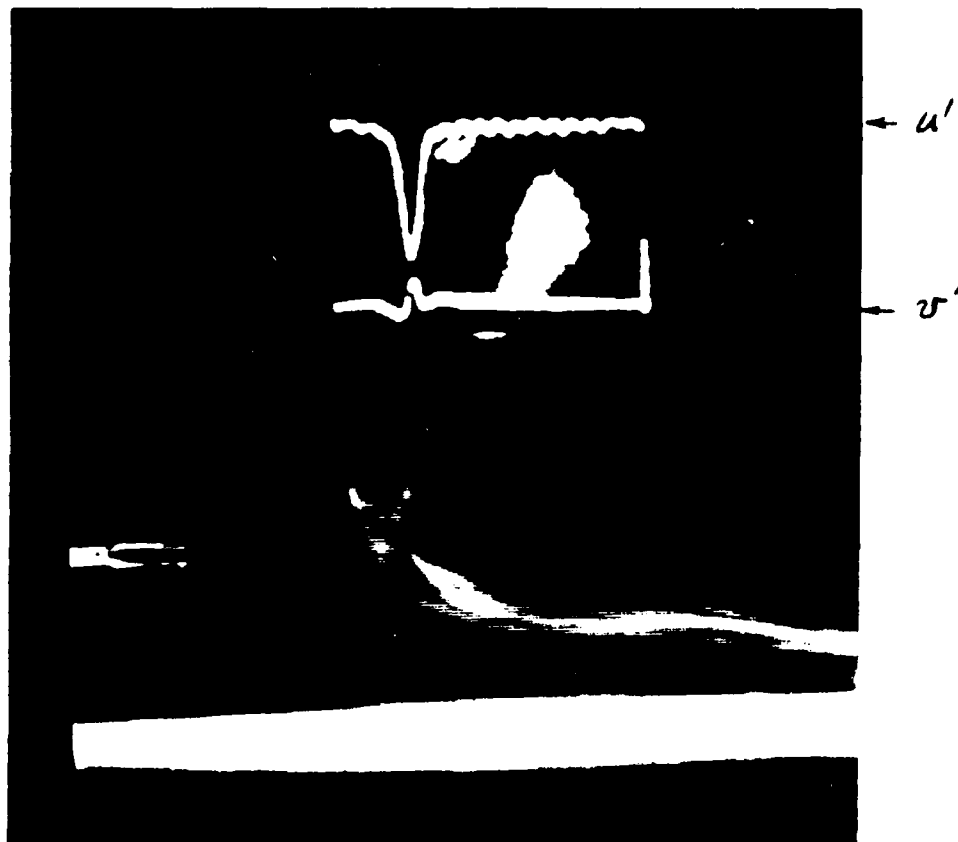
Fig. 18. Side view of single loop, showing signals recorded by hot-wire probe.
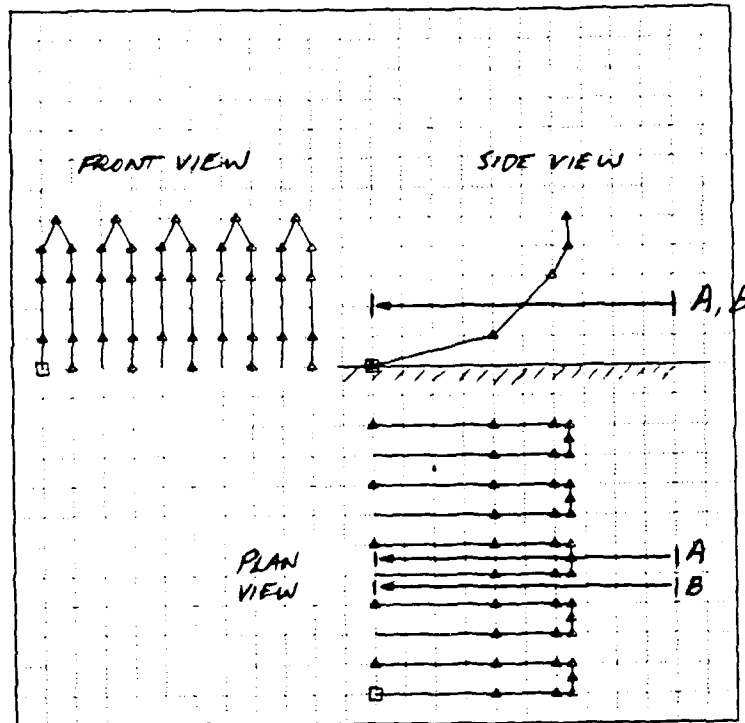
Fig. 19. Model of vortex loop array.
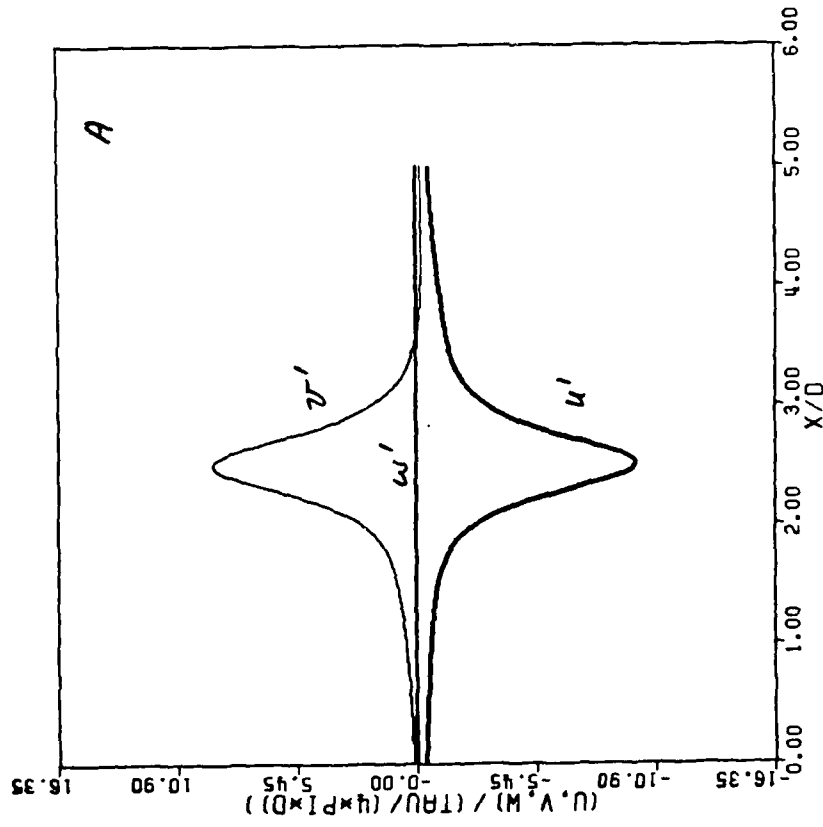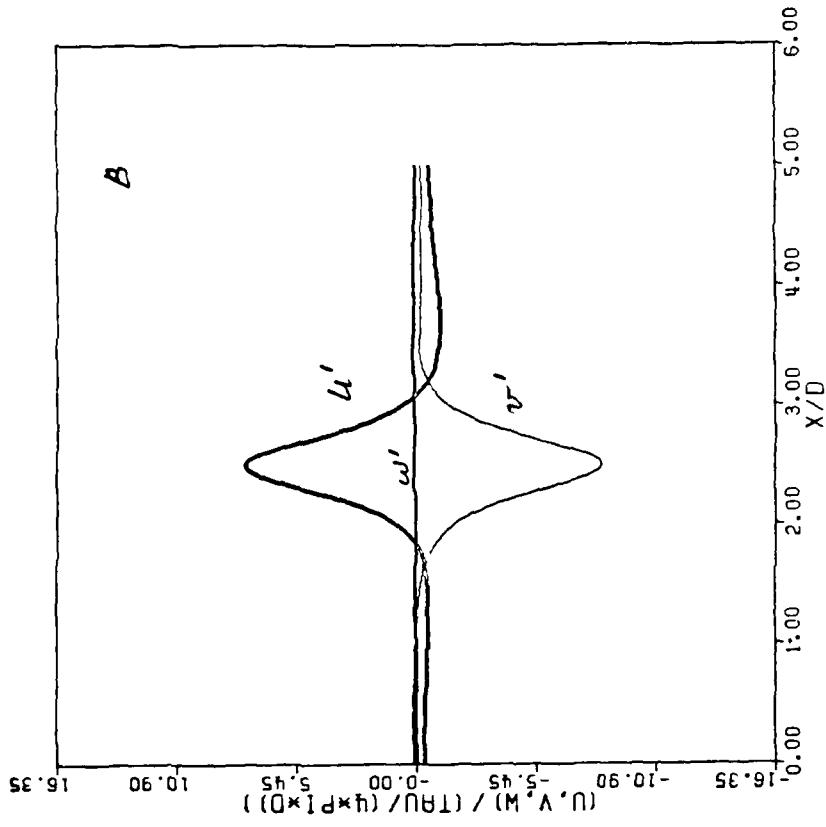
Fig. 20. **Signals of u' and v' as seen by observers at A and B in Fig. 13 as the loops convect past at constant speed.**
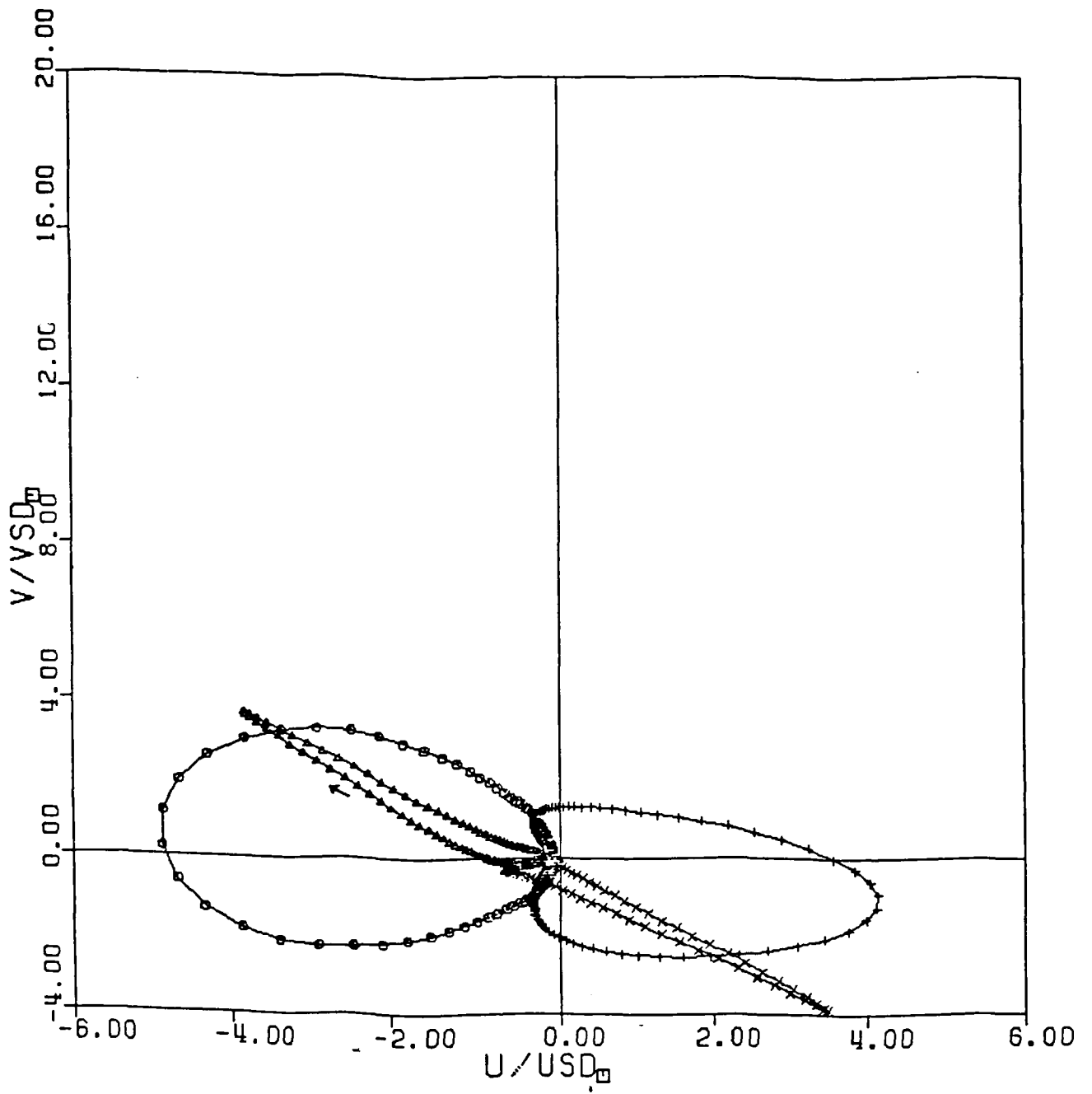
Fig. 21. Loci on the u-v plane for the signals seen by observers at A and B
in Fig. 19.

END

12 - 87

DTIC